

# Effects of variability of X-ray binaries on the X-ray luminosity functions of Milky Way

Nazma Islam<sup>a,b,\*</sup>, Biswajit Paul<sup>a</sup>

<sup>a</sup>*Raman Research Institute, C. V. Raman Avenue, Sadashivanagar, Bangalore-560012, India*

<sup>b</sup>*Joint Astronomy Programme, Indian Institute of Science, Bangalore-560012, India*

---

## Abstract

The X-ray luminosity functions of galaxies have become a useful tool for population studies of X-ray binaries in them. The availability of long term light-curves of X-ray binaries with the All Sky X-ray Monitors opens up the possibility of constructing X-ray luminosity functions, by also including the intensity variation effects of the galactic X-ray binaries. We have constructed multiple realizations of the X-ray luminosity functions (XLFs) of Milky Way, using the long term light-curves of sources obtained in the 2-10 keV energy band with the *RXTE*-ASM. The observed spread seen in the value of slope of both HMXB and LMXB XLFs are due to inclusion of variable luminosities of X-ray binaries in construction of these XLFs as well as finite sample effects. XLFs constructed for galactic HMXBs in the luminosity range  $10^{36} - 10^{39}$  erg/sec is described by a power-law model with a mean power-law index of -0.48 and a spread due to variability of HMXBs as 0.19. XLFs constructed for galactic LMXBs in the luminosity range  $10^{36} - 10^{39}$  erg/sec has a shape of cut-off power-law with mean power-law index of -0.31 and a spread due to variability of LMXBs as 0.07.

**Keywords:** X-rays: binaries; X-rays: galaxies; Galaxies: luminosity functions; Galaxies: Milky Way

---

X-ray emission from a normal galaxy i.e in absence of an AGN or X-ray emitting hot gas, is dominated by collective emission from its X-ray emitting point sources (Fabbiano, 2006). With the advent of *Chandra* and *XMM-Newton* X-ray telescopes era, detailed study of X-ray emission from nearby galaxies is now possible, and has further led to the identification of X-ray binaries in them. This in turn, has helped in construction of X-ray luminosity functions (XLFs) of such galaxies. These XLFs can also act as the indicators of star formation rate, stellar mass and evolution of these galaxies (Grimm et al., 2003; Ranalli et al., 2003; Gilfanov, 2004; Mineo et al., 2012; Kim and Fabbiano, 2010). In spite

---

\*Corresponding author

Email address: nazma@rri.res.in (Nazma Islam )

of the high angular resolution and sensitivity of these X-ray telescopes, the large distances to these galaxies limits us to probe higher luminosity end of their X-ray binary population. On the contrary, X-ray luminosity functions over a wide luminosities range can be constructed with the galactic X-ray binaries, the main hurdle of such an attempt being the distance uncertainty to these galactic sources. Initial attempts in constructing Log N-Log S relation for galactic X-ray binaries were made using X-ray sources from *Uhuru* catalog (Matilsky et al., 1973) and *ASCA* survey (Ogasaka et al., 1998; Sugizaki et al., 2001). Grimm et al. (2002) had constructed XLFs for X-ray binaries in Milky Way by averaging over their count-rates with the first five years of data of the *RXTE* All Sky Monitor. Galactic X-ray luminosity functions are also constructed using 15-50 keV *Swift*-BAT (Voss and Ajello, 2010) and 17-60 keV *INTEGRAL* surveys (Revnivtsev et al., 2008; Lutovinov et al., 2013).

However, the X-ray binaries are highly variable and are often unpredictable. The X-ray binaries show intensity variations by a large factor of a few to several orders of magnitude at all timescales above milliseconds. The galactic HMXB population is dominated by Be-HMXBs, in which the accretion onto the compact object occurs via formation of equatorial disc by stellar wind (Reig, 2011). These Be-HMXBs are usually quiescent and occasionally undergo outburst, during which their X-ray luminosity increases by several orders of magnitude. Supergiant HMXBs are another class of HMXB population, where the accretion onto the compact object occurs via a stellar wind or Roche-lobe overflow of the companion star. The galactic low mass X-ray binaries population are dominated by neutron star LMXBs, where the accretion onto the neutron star occurs via Roche Lobe overflow. These systems undergo thermonuclear X-ray bursts lasting few tens to hundreds of seconds (Galloway et al., 2008), superbursts lasting up to few hours and outbursts lasting few weeks to few months (Campana et al., 1998). The galactic low mass X-ray binaries population also consists of an appreciable number of Black hole LMXBs, most of which are transient in nature. During quiescence, they occupy very low luminosity states and occasionally they go into outbursts (novae), during which their luminosities increase by several orders of magnitude and they occupy very high luminosity states for a considerable period of time (Remillard and McClintock, 2006).

Multiple *Chandra* and *XMM*-Newton observations show that a large fraction of sources in external galaxies are also variable and includes many transient sources (Voss and Gilfanov, 2007; Williams et al., 2006). The X-ray luminosity functions for external galaxies are constructed out of tens of kilosec exposure of *Chandra* and *XMM*-Newton X-ray telescopes, which are essentially snapshot observations of extragalactic X-ray binaries. However, the galactic XLFs constructed by averaging luminosities of galactic X-ray binaries over 5 years of *RXTE*-ASM observations (Grimm et al., 2002), do not represent the true positions of X-ray binaries luminosities. It is now possible to construct XLFs of Milky Way, taking into account the variability of X-ray binaries because of the availability of long term light-curves of X-ray binaries in our Galaxy with *RXTE*-ASM.

The aim of the present work is to construct X-ray luminosity functions of

Milky Way taking into account the variable nature of the galactic X-ray binaries. We have used 16 years of *RXTE*–ASM data to construct differential and integral probability distributions of count-rates for X-ray binaries. Using this, we have constructed multiple realizations of X-ray luminosity functions of Milky Way. The X-ray luminosity functions, including completeness corrections for flux limited nature of ASM, are constructed separately for HMXBs and LMXBs and are fitted with power-law and power-law with cut-off respectively for each realization. These parameter values for multiple realizations are analyzed to estimate the effect of variability of X-ray binaries on the XLFs of Milky Way.

## 1. Data and Analysis

### 1.1. *RXTE All Sky Monitor light curves*

In order to construct X-ray luminosity functions of Milky Way including the effects of variability of X-ray binaries, long term light-curves of these sources are required. The long term light-curves obtained with the *RXTE* All Sky Monitor are useful due to all sky nature of its operation and long operational time of 16 years. It had three coded mask telescopes, was sensitive in 2-10 keV energy band and had a sky coverage of 80% in every 90 minutes (Levine et al., 1996). The sources in the ASM catalogue satisfy the criterion that they have reached an intensity of at least 5 mCrab in the operational time of *RXTE*–ASM and this catalogue excludes some sources like the highly absorbed, hard X-ray sources found in other catalogues like *Swift*–BAT, *INTEGRAL*–IBIS etc. The light-curves of the sources are obtained from *RXTE*–ASM archival data.<sup>1</sup>

### 1.2. *Luminosity functions and Variability effects*

#### 1.2.1. *Construction of differential and integral probability distributions of count-rates*

The cumulative X-ray luminosity function (XLF) for the X-ray binary population in a galaxy is defined as the number distribution  $N(> L)$  of X-ray binaries in a galaxy with luminosity greater than  $L$ , which is used throughout this paper. The X-ray luminosity functions for the Milky Way are constructed separately for 84 High Mass X ray Binaries and 116 Low Mass X ray Binaries whose distances are found in literature with reasonable accuracy (given in **Appendix** along with references). The light-curves of these sources are extracted from the dwell light-curves and are binned with 1 day bin time.

We quantify the variability in luminosities of each sources in the following way. We first determine the frequency of occurrence of each count rate, taking into account the errors in the count-rate given in the one day binned light-curve of each source. The errors on the count-rate in *RXTE*–ASM data consists of counting statistics along with systematic errors. For the same value of count-rate of a source, we see different values of errors in the ASM light-curves, which

---

<sup>1</sup>([ftp://heasarc.gsfc.nasa.gov/xte/data/archive/ASMPProducts/definitive\\_1dwell/lightcurves/](ftp://heasarc.gsfc.nasa.gov/xte/data/archive/ASMPProducts/definitive_1dwell/lightcurves/)).

makes it difficult to implement Maximum Likelihood method for determination of distribution of sources in presence of systematic errors, in the form suggested by Murdoch et al. (1973). Though it is not clear if the errors in the ASM light curve are gaussian, in the absence of any obvious alternative and for the sake of simplicity, the errors are assumed to be normally distributed for each count-rate. The true count-rate of the source corresponding to each data point in the light-curve, is then assumed to be normally distributed with the observed count rate as the mean of the distribution and the error associated with the count-rate as  $\sigma$  of the gaussian distribution.

To find the probability distribution corresponding to true count-rate, the gaussian distribution of each data point are integrated and summed up for all events as given by Equation.1.

$$y(a) = \frac{1}{N} \sum_{i=1}^N \frac{1}{\sqrt{2\pi}\sigma_i} \int_{a-0.05}^{a+0.05} \exp\left[-\frac{(x-c_i)^2}{2\sigma_i^2}\right] dx \quad (1)$$

where N is the total number of data points in one day binned light-curve,  $c_i$  is the  $i^{th}$  count rate,  $\sigma_i$  is the error associated with each  $c_i$  and a is the true count-rate bin along x-axis. The bin step for integration is taken to be 0.1 ASM count-rate and the integration for every true count-rate is carried out from half of the bin step preceding the count-rate (a-0.05) to half of the bin step after the count-rate (a+0.05).

The probability distribution of count-rates extending below zero obtained by this method are summed up for all data-points and is taken to be zero. The events which are registered as NULL in the ASM count rate, are neglected in the analysis. These events indicate the absence of any measurement for example, if the source is close to the Sun.

The probability distribution of count-rates constructed by this procedure is called differential probability distribution. From differential probability distribution, integral probability distribution is constructed which denotes the probability distribution of a source having count-rate greater than the  $c_x$  (count-rate bin along X axis).

The differential and integral probability distributions are constructed for 84 High Mass X ray Binaries and 116 Low Mass X ray Binaries (including field LMXBs as well as Globular clusters LMXBs). The distributions along with their light curves are shown for Cyg X-1 and Cyg X-3 in Figure. 1. In Figure. 1, the middle panel shows the comparison between differential probability distribution for the Cyg X-1 and Cyg X-3 and binned differential histogram of count-rates without accounting for errors on the count-rates.

A uniformly distributed random number between 0 and 1 is then compared with the integral probability distribution of each source and the corresponding count-rate is selected. The one day binned ASM count rate is converted to flux

by assuming a Crab-like spectrum for the sources and using the observed Crab count rate. The Crab flux of  $2.4 \times 10^{-8} \text{ erg cm}^{-2} \text{ s}^{-1}$  gives a count-rate of 75 counts/sec in 2-10 keV band of *RXTE*-ASM and is used for count-rate to flux conversion as given in Equation. 2 (Grimm et al., 2002).

$$F[\text{erg s}^{-1} \text{cm}^{-2}] = 3.2 \times 10^{-10} \cdot R[\text{counts s}^{-1}] \quad (2)$$

The flux of the sources determined by Equation. 2 are then converted to luminosities with their distances (given in **Appendix**), assuming an isotropic emission.

This process is repeated for each HMXB and LMXB sources and the corresponding selected luminosities are then used in construction of X ray luminosity distributions for one iteration. The XLFs constructed in this procedure are equivalent to XLFs constructed for snapshot observations of Milky Way from the viewpoint of an outside observer.

### 1.2.2. Completeness Correction

Due to the flux limited nature of the ASM sample and the incompleteness in the distance measurements to the X-ray binaries, the X-ray luminosity distribution derived in the previous section needs to be corrected for the X-ray binaries not visible to ASM. To account for the completeness of the sample, we have used the same model of spatial distribution of X-ray binaries as mentioned in Grimm et al. (2002). The HMXB spatial distribution is modeled by disk density distribution parameterized in Dehnen and Binney (1998), with 100% modulation by galactic spiral arms densities (spiral arms computed from Taylor and Cordes 1993). The LMXB spatial distribution is modeled by three component model of Bahcall and Soneira (1980), where the parameters of bulge, disk and spheroid were appropriately chosen to fit the observed LMXB distribution. The LMXB disk density distribution was 20% modulated by the galactic spiral arm densities. The various parameters of the Galaxy model are tabulated in Table.(4) of Grimm et al. (2002).

From Equation. 3 taken from Grimm et al. (2002)

$$\left(\frac{dN}{dL}\right)_{obs} = \left(\frac{dN}{dL}\right) \times \left(\frac{M(< D(L))}{M_{tot}}\right) \quad (3)$$

where  $\frac{dN}{dL}$  is the true luminosity function,  $\left(\frac{dN}{dL}\right)_{obs}$  is the flux luminosity distribution constructed from snapshot *RXTE*-ASM measurements and  $\left(\frac{M(< D(L))}{M_{tot}}\right)$  is the fraction of mass visible to ASM on account of flux limitation and distance incompleteness beyond 10 kpc. From Figure.11 of Grimm et al. (2002), which plots the fraction of mass of the galaxy visible to ASM as a function of luminosities, both the LMXB and HMXB mass fraction has a flat part of the curve above  $10^{36} \text{ ergs/s}$ . Below  $10^{36} \text{ ergs/s}$ , the mass fraction of both LMXBs and HMXBs visible to ASM rapidly decreases. To avoid any artifacts in the snapshot luminosity functions and to ensure that the change in the parameters of the luminosity functions is introduced by the luminosity variations in the sources alone, we have constructed the galactic X-ray luminosity functions from

$10^{36}$  to  $10^{39}$  ergs/sec luminosity regime (flat part of the mass fraction of galaxy visible to ASM).

### 1.2.3. Construction of Snapshot Observations

The randomly selected luminosities of all HMXBs and LMXBs sources in one iteration are used to determine the parameters of X-ray luminosity functions for one snapshot observation. Using the same model functions as used in Grimm et al. (2002), the HMXB distribution is then fitted with a power-law in luminosity range  $10^{36} - 10^{39}$  erg/s.

$$N(> L) = K \cdot \left(\frac{L}{10^{36}}\right)^{-a} \quad (4)$$

The LMXB distribution is fitted with a power-law with a cut-off in the luminosity range  $10^{36} - 10^{39}$  erg/s.

$$N(> L) = K \cdot \left[\left(\frac{L}{10^{36}}\right)^{-a} - \left(\frac{L_{max}}{10^{36}}\right)^{-a}\right] \quad (5)$$

We calculate the best fit values of the parameters by using the Maximum-Likelihood (ML) method in the form suggested by Crawford et al. (1970). The main advantage of using this implementation of ML is that we use ungrouped data (luminosities) in parameter estimation. The value of slope of the power-law (power-law with a cut-off in case of LMXB) is calculated by solving the following equation (Crawford et al., 1970)

$$\frac{M}{a} - \sum_i \ln s_i - \frac{M \ln b}{b^a - 1} = 0 \quad (6)$$

where M is the total number of HMXB or LMXB sources in a snapshot observations having luminosity greater than  $10^{36}$  ergs/sec,  $s_i$  is the luminosities of each source in units of  $10^{36}$  and b (in units of  $10^{36}$ ) is the maximum value of luminosity present in each iteration. The statistical error on slope  $a$  is (Crawford et al., 1970)

$$\Sigma_a = \frac{a}{\sqrt{M}} \left(1 - \frac{a^2 (\ln b)^2}{b^a}\right)^{-\frac{1}{2}} \quad (7)$$

As mentioned in Grimm et al. (2002), the cut-off of the LMXB distribution is taken as the maximum luminosity of the sample in a given iteration. The normalisation K of the HMXB XLFs for a given iteration is taken to be the number of sources (including completeness corrections obtained from Figure.11 of Grimm et al. (2002)) having luminosities greater than  $10^{36}$  ergs/sec. For the LMXB XLFs, it is the number of sources (including completeness corrections obtained from Figure.11 of Grimm et al. (2002)) greater than  $10^{36}$  ergs/sec divided by  $(1 - L_{max}^{-a})$ . A plot of the XLF and the best fit model for one arbitrarily chosen iteration, without and with completeness corrections, is shown for HMXBs and LMXBs in Figure. 2.

Using different seeds in the random number generator, the above process is repeated 10,000 times and for each iteration, different values of slopes are

obtained from Equation. 6 along with its statistical error. The parameter values obtained for different iterations are plotted as histograms. The mean value and standard deviation ( $\sigma$ ) of parameters are calculated from their respective histograms. The mean values of parameters along with their  $\sigma$  are tabulated in Table. 1 and the histogram of parameters are shown in Figure. 3 for LMXB XLFs and HMXB XLFs respectively. We have also calculated the mean of statistical error  $\Sigma_a$  on the values of slopes for each iteration.

To determine the goodness of fit of models given by Equation. 4 to the HMXB XLFs and Equation. 5 to the LMXB XLFs, we have performed Kolmogorov-Smirnoff test (KS test) on the data and compared it with its respective model. The average KS probability ( $p$ ) value for 10000 iterations of HMXB XLFs is  $\sim 0.44$  and the average  $p$  value for 10000 iterations of LMXB XLFs is  $\sim 0.41$ . Out of the total 10000 iterations for each type, 9359 of the HMXB XLFs and 9548 of the LMXB XLFs have  $p > 0.1$ .

## 2. Discussions and Conclusions

Previous work by Grimm et al. (2002) had utilized the first 5 years of *RXTE*-ASM data for constructing the averaged XLFs separately using 25 HMXBs and 84 LMXBs. However, these galactic XLFs do not include the variability effects of X-ray binaries and for a transient X-ray binary, the averaged count-rates do not represent the true positions of such systems in the XLF. Therefore, we have used 16 years light-curves of 2-10 keV energy band of *RXTE*-ASM of 84 HMXBs and 116 LMXBs to construct multiple realizations of the XLFs for the Milky Way by incorporating the variable nature of X-ray binaries. The differential and integral probability distributions of count-rates in 2-10 keV *RXTE*-ASM light-curves are constructed for each source. The snapshot luminosity distribution are constructed separately for galactic HMXBs and LMXBs and includes completeness corrections for flux limited nature of ASM sample. For each iteration of the HMXBs, the XLF is fitted with a power-law, whereas for the LMXBs, the XLF is fitted with a power-law with cut-off. The value of slope of the power-law and power-law with cut-off is estimated from Maximum Likelihood analysis, along with the statistical error on the value of slope. This process is repeated for 10,000 realizations of XLFs of Milky Way and obtain values of XLFs parameters for all these realizations. The mean and  $\sigma$  of each parameter is estimated from these values of 10,000 realizations. For each realization, we also obtain the statistical error on the value of slope  $\Sigma_a$ , which is then averaged.

The HMXB luminosity function taking into account variability of High Mass X-ray binaries, in luminosity range  $10^{36} - 10^{39}$  erg/s is given by:

$$N(> L) = (54 \pm 8) \left( \frac{L}{10^{36} \text{ erg/s}} \right)^{-(0.48 \pm 0.19)} \quad (8)$$

The LMXB luminosity function taking into account the variability of Low Mass X-ray binaries, in luminosity range  $10^{36} - 10^{39}$  erg/s is given by:

$$N(> L) = (127 \pm 8) \left( \frac{L}{10^{36} \text{ erg/s}} \right)^{-(0.31 \pm 0.07)} - ((4.28 \pm 1.6) \times 10^3)^{-(0.31 \pm 0.07)} \quad (9)$$

The value of  $\sigma$  quoted here as the spread in the value of slope for the HMXB and LMXB luminosity functions is mainly due to the variations in the XLFs arising from the variability effects of X-ray binaries. This is different from the statistical error on the value of slope  $\Sigma_a$ , given in Equation. 7, arising due to finite N sample effects. As seen in Table.1, the spread in the slope seen due to variability of X-ray binaries is marginally larger than the averaged  $\Sigma_a$  for both HMXB and LMXB XLFs.

For LMXB distribution, the most luminous source in X-rays for a given iteration determines the cut-off of the distribution. The most luminous and persistent LMXB X-ray source in 2-10 keV energy band of *RXTE*-ASM in our Galaxy is Sco X-1, which determines the cut-off of LMXB distribution for a majority of the snapshots. However, some of the galactic LMXB transients (like Aql X-1 and other Black hole binaries like GRS 1915+105) during outbursts occasionally outshines Sco X-1, which in turn influences the cut-off of the LMXB distribution for the snapshots in which such luminosities are included. As shown in Table. 1, the cut-off of the LMXB distribution is of the order of Eddington luminosity for  $1.4 M_\odot$  He accreting neutron star LMXB.

The slope of the LMXB XLF is similar to that found in previous study by Grimm et al. (2002). However, the slope of the HMXB XLF is smaller than that of HMXB XLF given in Grimm et al. (2002). This discrepancy could be due to inclusion of more Be-HMXBs in the sample, which have high luminosity during the outbursts and are non-detectable with ASM during their quiescence. Also HMXBs like LSI +61303, X Per and Supergiant Fast X-ray Transients like IGR J18483-0311, are included in some snapshot observations when they are in high luminosity states.

From Figure. 3, we see that the slope histogram of HMXB XLFs have a larger spread than the slope histogram of LMXB XLFs. Since two-thirds of the galactic HMXB population consists of Be-HMXBs and HMXB XLFs are mostly influenced by the collective emission properties of these stellar wind driven Be-HMXB systems, we can infer that a large fraction of transients in the underlying population of HMXBs leads to larger spread in HMXB XLFs than that seen in LMXB XLFs. Postnov (2003) and Bhadkamkar and Ghosh (2012) have shown that the power law shape of the HMXB XLF can be explained by the stellar wind properties of massive stars. Most of the HMXBs systems are NS-HMXBs, with only 6 HMXB having black holes. Cyg X-1 and Cyg X-3 are the most luminous HMXB systems and therefore always occupy higher end of HMXB XLFs.

The LMXB population consists of both field LMXBs as well as Globular Clusters (GCs) LMXBs. The LMXBs in GCs have different XLF behaviour compared to field LMXBs as seen in the study of LMXBs in the bulge of M 31 (Voss and Gilfanov, 2007). Since there are only 12 LMXBs in the catalogue of galactic LMXBs (Liu et al., 2007), we have ignored the possible effects of



LMXBs in GCs on the LMXB XLFs. The LMXB XLFs are mostly influenced by the collective emission properties of these NS-LMXBs with the break in the XLF either due to the change in the mass transfer rate in the binary systems (Postnov and Kuranov, 2005) or due to fraction of Giant donors in population of LMXBs (Revnivtsev et al., 2011). There are also an appreciable number of transient BH LMXBs, which are either in quiescence and occupy very low luminosity states or undergo outbursts for a brief period of time and occupy high luminosity end of XLFs.

In this paper, we have probed one aspect of probable variation in XLFs due to variable nature of X-ray binaries. In case of star-bursts galaxies, the number of HMXBs present in a galaxy is related to its Star Formation Rate (SFR), whereas for elliptical galaxies, the number of LMXBs present in a galaxy is related to its stellar mass (Mineo et al., 2012). It will be interesting to probe the variation in extra-galactic XLFs due to both variability of X-ray binaries as well as the number of X-ray binaries present, which differs from galaxy to galaxy.

#### ACKNOWLEDGMENT

This research has made use of quick-look results of *RXTE*–ASM obtained through High Energy Astrophysics Science Archive Research Center Online Service (HEASARC), provided by the NASA/Goddard Space Flight Center. We thank Shiv Sethi and Harshal Bhadkamkar for useful discussions.

#### References

- Bahcall, J. N., Soneira, R. M., Sep. 1980. The universe at faint magnitudes. I - Models for the galaxy and the predicted star counts. *ApJS* 44, 73–110.
- Bhadkamkar, H., Ghosh, P., Feb. 2012. Collective Properties of X-Ray Binary Populations of Galaxies. I. Luminosity and Orbital Period Distributions of High-mass X-Ray Binaries. *ApJ* 746, 22.
- Bodaghee, A., Tomsick, J. A., Rodriguez, J., James, J. B., Jan. 2012. Clustering between High-mass X-Ray Binaries and OB Associations in the Milky Way. *ApJ* 744, 108.
- Campana, S., Colpi, M., Mereghetti, S., Stella, L., Tavani, M., 1998. The neutron stars of Soft X-ray Transients. *A&A Rev.* 8, 279–316.
- Coleiro, A., Chaty, S., Feb. 2013. Distribution of High-mass X-Ray Binaries in the Milky Way. *ApJ* 764, 185.
- Crawford, D. F., Jauncey, D. L., Murdoch, H. S., Nov. 1970. Maximum-Likelihood Estimation of the Slope from Number-Flux Counts of Radio Sources. *ApJ* 162, 405.

- Dehnen, W., Binney, J., Mar. 1998. Mass models of the Milky Way. *MNRAS* 294, 429.
- Fabbiano, G., Sep. 2006. Populations of X-Ray Sources in Galaxies. *ARA&A* 44, 323–366.
- Galloway, D. K., Muno, M. P., Hartman, J. M., Psaltis, D., Chakrabarty, D., Dec. 2008. Thermonuclear (Type I) X-Ray Bursts Observed by the Rossi X-Ray Timing Explorer. *ApJS* 179, 360–422.
- Gilfanov, M., Mar. 2004. Low-mass X-ray binaries as a stellar mass indicator for the host galaxy. *MNRAS* 349, 146–168.
- Grimm, H.-J., Gilfanov, M., Sunyaev, R., Sep. 2002. The Milky Way in X-rays for an outside observer. Log(N)-Log(S) and luminosity function of X-ray binaries from RXTE/ASM data. *A&A* 391, 923–944.
- Grimm, H.-J., Gilfanov, M., Sunyaev, R., Mar. 2003. High-mass X-ray binaries as a star formation rate indicator in distant galaxies. *MNRAS* 339, 793–809.
- Jonker, P. G., Nelemans, G., Oct. 2004. The distances to Galactic low-mass X-ray binaries: consequences for black hole luminosities and kicks. *MNRAS* 354, 355–366.
- Kim, D.-W., Fabbiano, G., Oct. 2010. X-ray Properties of Young Early-type Galaxies. I. X-ray Luminosity Function of Low-mass X-ray Binaries. *ApJ* 721, 1523–1530.
- Levine, A. M., Bradt, H., Cui, W., Jernigan, J. G., Morgan, E. H., Remillard, R., Shirey, R. E., Smith, D. A., Sep. 1996. First Results from the All-Sky Monitor on the Rossi X-Ray Timing Explorer. *ApJ* 469, L33.
- Liu, Q. Z., van Paradijs, J., van den Heuvel, E. P. J., Mar. 2001. A catalogue of low-mass X-ray binaries. *A&A* 368, 1021–1054.
- Liu, Q. Z., van Paradijs, J., van den Heuvel, E. P. J., Sep. 2006. Catalogue of high-mass X-ray binaries in the Galaxy (4th edition). *A&A* 455, 1165–1168.
- Liu, Q. Z., van Paradijs, J., van den Heuvel, E. P. J., Jul. 2007. A catalogue of low-mass X-ray binaries in the Galaxy, LMC, and SMC (Fourth edition). *A&A* 469, 807–810.
- Lutovinov, A. A., Revnivtsev, M. G., Tsygankov, S. S., Krivonos, R. A., May 2013. Population of persistent high-mass X-ray binaries in the Milky Way. *MNRAS* 431, 327–341.
- Matilsky, T., Gursky, H., Kellogg, E., Tananbaum, H., Murray, S., Giacconi, R., May 1973. The Number-Intensity Distribution of X-Ray Sources Observed by UHURU. *ApJ* 181, 753–760.

- Mineo, S., Gilfanov, M., Sunyaev, R., Jan. 2012. X-ray emission from star-forming galaxies - I. High-mass X-ray binaries. *MNRAS* 419, 2095–2115.
- Murdoch, H. S., Crawford, D. F., Jauncey, D. L., Jul. 1973. Maximum-Likelihood Estimation of the Number-Flux Distribution of Radio Sources in the Presence of Noise and Confusion. *ApJ* 183, 1–14.
- Negueruela, I., Oct. 1998. On the nature of Be/X-ray binaries. *A&A* 338, 505–510.
- Ogasaka, Y., Kii, T., Ueda, Y., Takahashi, T., Yamada, T., Inoue, H., Ishisaki, Y., Ohta, K., Makishima, K., Miyaji, T., Hasinger, G., 1998. Sky surveys with ASCA — Deep Sky Survey. *Astronomische Nachrichten* 319, 43.
- Postnov, K. A., Jun. 2003. The Universal Luminosity Function of Binary X-ray Sources in Galaxies. *Astronomy Letters* 29, 372–373.
- Postnov, K. A., Kuranov, A. G., Jan. 2005. The Luminosity Function of Low-Mass X-ray Binaries in Galaxies. *Astronomy Letters* 31, 7–14.
- Ranalli, P., Comastri, A., Setti, G., Feb. 2003. The 2–10 keV luminosity as a Star Formation Rate indicator. *A&A* 399, 39–50.
- Reig, P., Mar. 2011. Be/X-ray binaries. *Ap&SS* 332, 1–29.
- Remillard, R. A., McClintock, J. E., Sep. 2006. X-Ray Properties of Black-Hole Binaries. *ARA&A* 44, 49–92.
- Revnivtsev, M., Lutovinov, A., Churazov, E., Sazonov, S., Gilfanov, M., Grebenev, S., Sunyaev, R., Nov. 2008. Low-mass X-ray binaries in the bulge of the Milky Way. *A&A* 491, 209–217.
- Revnivtsev, M., Postnov, K., Kuranov, A., Ritter, H., Feb. 2011. On the nature of the break in the X-ray luminosity function of low-mass X-ray binaries. *A&A* 526, A94.
- Reynolds, A. P., Quaintrell, H., Still, M. D., Roche, P., Chakrabarty, D., Levine, S. E., Jun. 1997. A new mass estimate for Hercules X-1. *MNRAS* 288, 43–52.
- Sugizaki, M., Mitsuda, K., Kaneda, H., Matsuzaki, K., Yamauchi, S., Koyama, K., May 2001. Faint X-Ray Sources Resolved in the ASCA Galactic Plane Survey and Their Contribution to the Galactic Ridge X-Ray Emission. *ApJS* 134, 77–102.
- Taylor, J. H., Cordes, J. M., Jul. 1993. Pulsar distances and the galactic distribution of free electrons. *ApJ* 411, 674–684.
- Torrejón, J. M., Negueruela, I., Smith, D. M., Harrison, T. E., Feb. 2010. Near-infrared survey of high mass X-ray binary candidates. *A&A* 510, A61.

- van Paradijs, J., White, N., Jul. 1995. The Galactic Distribution of Low-Mass X-Ray Binaries. *ApJ* 447, L33.
- Voss, R., Ajello, M., Oct. 2010. Swift-BAT Survey of Galactic Sources: Catalog and Properties of the Populations. *ApJ* 721, 1843–1852.
- Voss, R., Gilfanov, M., Jun. 2007. A study of the population of LMXBs in the bulge of M 31. *A&A* 468, 49–59.
- Williams, B. F., Naik, S., Garcia, M. R., Callanan, P. J., May 2006. A Catalog of Transient X-Ray Sources in M31. *ApJ* 643, 356–375.
- Wu, Y. X., Yu, W., Li, T. P., Maccarone, T. J., Li, X. D., Aug. 2010. Orbital Period and Outburst Luminosity of Transient Low Mass X-ray Binaries. *ApJ* 718, 620–631.

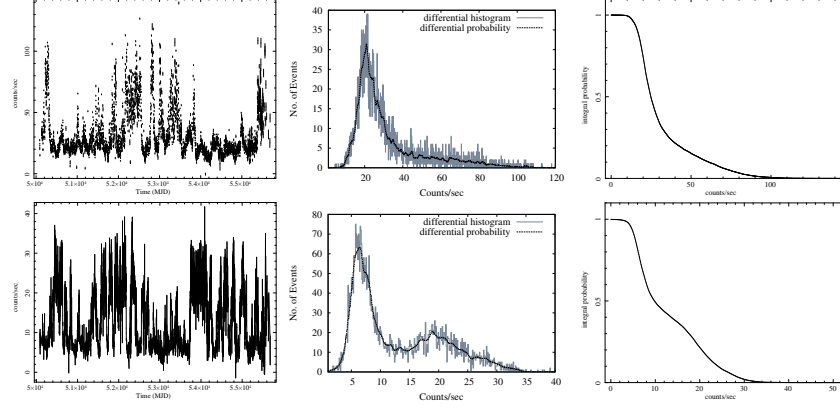


**Figure 1:** Light curve of Cyg X-1 (upper left panel) and Cyg X-3 (lower left panel), comparison between differential probability distribution and differential histogram (upper middle panel for Cyg X-1 and lower middle panel for Cyg X-3) and integral probability distribution (upper right panel for Cyg X-1 and lower right panel for Cyg X-3) are shown here.

**Table 1:** Mean parameters values with their  $\sigma$  for 10,000 iterations.  $\Sigma_a$  is the averaged statistical error on the value of slope  $a$

Sample	$a$	$\sigma_a$	$\Sigma_a$	K	$\sigma_K$	$L_{max}$ ( $10^{38}$ ergs/sec)	$\sigma_{L_{max}}$ ( $10^{38}$ ergs/sec)
HMXB	0.48	0.19	0.11	54	8	-	-
LMXB	0.31	0.07	0.05	127	8	4.28	1.6

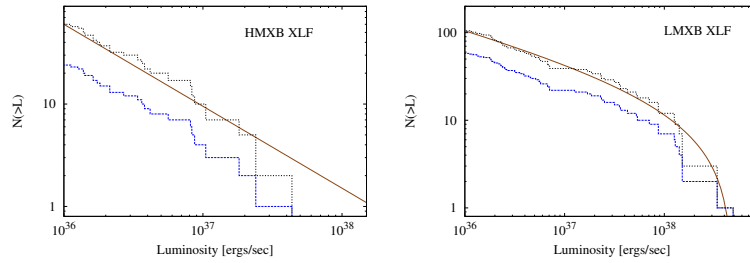


**Figure 2:** The observed (dashed line) and volume corrected (dotted line) Log N-Log L distribution of HMXB (left panel) and LMXB (right panel) for one arbitrarily chosen iteration. Solid line represents the best fit to the distribution with the parameter values obtained from M-L method, power-law model given by Equation. 4 for HMXBs and power-law with a cut-off model given by Equation. 5 for LMXBs.

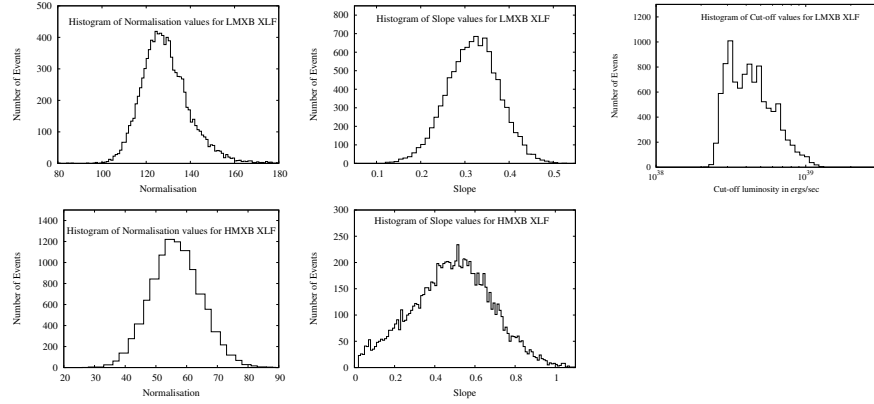


**Figure 3:** Histograms of LMXB XLFs and HMXB XLFs parameter values for 10,000 iterations. Top panel shows the distribution of Normalisation (left panel), Slope (middle panel) and Cut-off (right panel) of LMXB XLFs. Lower panel shows the distribution of Normalisation (left panel) and Slope (right panel) of HMXB XLFs.

### Appendix: Distances to X ray binaries

X ray sources	Distance(Kpc)	Type	References
AqlX-1	3.4	LMXB	van Paradijs and White (1995)
CirX-1	10.9	LMXB	van Paradijs and White (1995)
CygX-1	2.1	HMXB	Grimm et al. (2002)
CygX-2	11.3	LMXB	van Paradijs and White (1995)
CygX-3	9.0	HMXB	van Paradijs and White (1995)
EXO0748-676	7.6	LMXB	Galloway et al. (2008)
GROJ1744-28	8.5	LMXB	van Paradijs and White (1995)
GRS1915+105	12.5	LMXB	Grimm et al. (2002)
GS1124-684	5.5	LMXB	van Paradijs and White (1995)
GS1843+009	12.5	HMXB	Grimm et al. (2002)
GS2000+250	2.7	LMXB	Liu et al. (2007)
GS2023+338	4.3	LMXB	van Paradijs and White (1995)
GX5-1	7.2	LMXB	Grimm et al. (2002)
GX13+1	7.0	LMXB	Grimm et al. (2002)
GX17+2	9.5	LMXB	Galloway et al. (2008)
GX301-2	3.1	HMXB	Coleiro and Chaty (2013)
GX340+0	11.0	LMXB	van Paradijs and White (1995)
GX349+2	9.2	LMXB	Grimm et al. (2002)
GX354+0	5.7	HMXB	Grimm et al. (2002)
KS1731-260	5.6	LMXB	Galloway et al. (2008)
SerX-1	8.4	LMXB	Grimm et al. (2002)
V4641Sgr	9.9	HMXB	Grimm et al. (2002)
X1538-522	4.5	HMXB	Bodaghee et al. (2012)
X1608-522	4.0	LMXB	van Paradijs and White (1995)
X1624-490	13.5	LMXB	Grimm et al. (2002)
X1636-536	5.95	LMXB	Galloway et al. (2008)
X1657-415	7.1	HMXB	Bodaghee et al. (2012)
X1705-440	7.4	LMXB	Grimm et al. (2002)
X1715-321	6.1	HMXB	Grimm et al. (2002)
X1735-444	6.5	LMXB	Galloway et al. (2008)
X1812-121	3.8	HMXB	Grimm et al. (2002)
X1820-303	4.94	LMXB	Galloway et al. (2008)
X1905+000	7.7	HMXB	Grimm et al. (2002)
X1908+075	6.4	HMXB	Grimm et al. (2002)
X1916-053	6.8	LMXB	Galloway et al. (2008)
XTEJ1550-564	5.3	LMXB	Grimm et al. (2002)
X0115+634	5.3	HMXB	Coleiro and Chaty (2013)
RXJ0146.9+6121	2.3	HMXB	Negueruela (1998)
V0332+53	7.0	HMXB	Negueruela (1998)
X0535+262	3.8	HMXB	Coleiro and Chaty (2013)
X0726-260	5.0	HMXB	Coleiro and Chaty (2013)
GROJ1008-57	5.0	HMXB	Negueruela (1998)
X1118-616	3.2	HMXB	Coleiro and Chaty (2013)
X1145-619	4.3	HMXB	Coleiro and Chaty (2013)
X1417-624	7.0	HMXB	Coleiro and Chaty (2013)
EXO2030+375	3.1	HMXB	Coleiro and Chaty (2013)
CepX-4	3.7	HMXB	Coleiro and Chaty (2013)
ScoX-1	2.8	LMXB	Grimm et al. (2002)
X0836-426	8.2	LMXB	Galloway et al. (2008)
X0918-548	4.0	LMXB	Galloway et al. (2008)
X1254-690	15.5	LMXB	Galloway et al. (2008)
X1323-619	11.0	LMXB	Galloway et al. (2008)
X1702-429	4.19	LMXB	Galloway et al. (2008)
XTEJ1723-376	10.0	LMXB	Galloway et al. (2008)
X1724-307	5.0	LMXB	Galloway et al. (2008)
SL1735-269	5.6	LMXB	Galloway et al. (2008)

### Appendix: Distances to X ray binaries(continued)

X ray sources	Distance	Type	References
XTEJ1739-285	7.3	LMXB	Galloway et al. (2008)
SAXJ1747-2853	5.2	LMXB	Galloway et al. (2008)
IGRJ17473-2721	4.9	LMXB	Galloway et al. (2008)
SL1744-300	8.4	LMXB	Galloway et al. (2008)
GX3+1	5.0	LMXB	Galloway et al. (2008)
X1744-361	8.4	LMXB	Galloway et al. (2008)
EXO1745-248	4.73	LMXB	Galloway et al. (2008)
X1746-370	16.0	LMXB	Galloway et al. (2008)
SAXJ1750.8-2900	5.21	LMXB	Galloway et al. (2008)
GRS1747-312	9.0	LMXB	Galloway et al. (2008)
XTEJ1759-220	16.0	LMXB	Galloway et al. (2008)
SAXJ1808.4-3658	2.77	LMXB	Galloway et al. (2008)
XTEJ1814-338	7.9	LMXB	Galloway et al. (2008)
GS1826-238	6.7	LMXB	Galloway et al. (2008)
X1832-330	6.7	LMXB	Galloway et al. (2008)
HETEJ1900.1-2455	3.6	LMXB	Galloway et al. (2008)
XTEJ2123-058	14.0	LMXB	Galloway et al. (2008)
IGRJ18027-2017	12.4	HMXB	Torrejón et al. (2010)
SAXJ1818.6-1703	2.7	HMXB	Coleiro and Chaty (2013)
IGRJ18483-0311	2.83	HMXB	Torrejón et al. (2010)
IGRJ1914+0951	3.6	HMXB	Torrejón et al. (2010)
GROJ0422+32	2.5	LMXB	Jonker and Nelemans (2004)
X0620-003	1.2	LMXB	Jonker and Nelemans (2004)
GRS1009-45	5.7	LMXB	Jonker and Nelemans (2004)
XTEJ1118+480	1.8	LMXB	Jonker and Nelemans (2004)
X1543-475	7.5	LMXB	Jonker and Nelemans (2004)
GROJ1655-40	3.2	LMXB	Jonker and Nelemans (2004)
GX339-4	6.0	LMXB	Jonker and Nelemans (2004)
X1705-250	8.6	LMXB	Jonker and Nelemans (2004)
XTEJ1859+226	6.3	LMXB	Jonker and Nelemans (2004)
X1658-298	8.4	LMXB	Jonker and Nelemans (2004)
SAXJ1712.6-3739	5.9	LMXB	Jonker and Nelemans (2004)
RXJ1718.4-4029	6.4	LMXB	Jonker and Nelemans (2004)
SAXJ1810.8-2609	5.1	LMXB	Jonker and Nelemans (2004)
X0656-072	3.9	HMXB	Grimm et al. (2002)
X1354-644	27.0	LMXB	Wu et al. (2010)
XTEJ1650-500	2.6	LMXB	Wu et al. (2010)
IGRJ00291+5934	2.6	LMXB	Wu et al. (2010)
XTEJ0929-314	10.0	LMXB	Wu et al. (2010)
XTEJ1751-305	8.5	LMXB	Wu et al. (2010)
X0114+650	6.5	HMXB	Coleiro and Chaty (2013)
X1845-024	10.0	HMXB	Bodaghee et al. (2012)
X2206+543	3.4	HMXB	Coleiro and Chaty (2013)
X1700-377	1.8	HMXB	Coleiro and Chaty (2013)
AXJ1820.5-1434	8.2	HMXB	Bodaghee et al. (2012)
GammaCas	0.17	HMXB	Coleiro and Chaty (2013)
GX304-1	1.3	HMXB	Coleiro and Chaty (2013)
X1907+097	5.0	HMXB	Bodaghee et al. (2012)
RXJ0037.2+6121	3.0	HMXB	Bodaghee et al. (2012)
IGRJ01363+6610	2.0	HMXB	Bodaghee et al. (2012)
IGRJ01583+6713	4.1	HMXB	Coleiro and Chaty (2013)
IGRJ06074+2205	4.5	HMXB	Coleiro and Chaty (2013)
IGRJ08408-4503	3.4	HMXB	Coleiro and Chaty (2013)
IGRJ11215-5952	7.3	HMXB	Coleiro and Chaty (2013)
IGRJ11305-6252	3.6	HMXB	Coleiro and Chaty (2013)
IGRJ11435-6109	9.8	HMXB	Coleiro and Chaty (2013)



### Appendix: Distances to X ray binaries(continued)

X ray sources	Distance	Type	References
IGRJ16195-4945	4.5	HMXB	Bodaghee et al. (2012)
IGRJ16318-4848	1.6	HMXB	Bodaghee et al. (2012)
IGRJ16320-4751	3.5	HMXB	Bodaghee et al. (2012)
IGRJ16393-4643	10.6	HMXB	Bodaghee et al. (2012)
IGRJ16418-4532	13.0	HMXB	Bodaghee et al. (2012)
IGRJ16479-4514	2.8	HMXB	Bodaghee et al. (2012)
IGRJ17544-2619	3.2	HMXB	Bodaghee et al. (2012)
IGRJ18450-0435	6.4	HMXB	Coleiro and Chaty (2013)
KS1947+300	8.5	HMXB	Coleiro and Chaty (2013)
PSR1259-63	1.7	HMXB	Coleiro and Chaty (2013)
RXJ1826.2-1450	2.5	HMXB	Bodaghee et al. (2012)
SAXJ2103.5+4545	8.0	HMXB	Coleiro and Chaty (2013)
SS433	5.5	HMXB	Bodaghee et al. (2012)
SWIFTJ2000.6+3210	8.0	HMXB	Bodaghee et al. (2012)
VelaX-1	2.2	HMXB	Coleiro and Chaty (2013)
XPer	1.2	HMXB	Coleiro and Chaty (2013)
XTEJ1543-568	10.0	HMXB	Bodaghee et al. (2012)
XTEJ1810-189	11.5	HMXB	Bodaghee et al. (2012)
XTEJ1829-098	10.0	HMXB	Bodaghee et al. (2012)
XTEJ1855-026	10.8	HMXB	Coleiro and Chaty (2013)
X1145-616	8.5	HMXB	Bodaghee et al. (2012)
CenX-3	9.0	HMXB	Grimm et al. (2002)
CenX-4	1.6	HMXB	Grimm et al. (2002)
GRS1716-249	2.4	LMXB	Liu et al. (2001)
HK1732-304	5.2	LMXB	Liu et al. (2001)
1E1024.1-5733	3.0	HMXB	Grimm et al. (2002)
EXO1846-031	7.0	LMXB	Grimm et al. (2002)
GX9+1	7.2	LMXB	Grimm et al. (2002)
GX9+9	7.0	LMXB	Grimm et al. (2002)
LSI+61303	2.3	HMXB	Grimm et al. (2002)
RXJ0812.4-3115	8.6	HMXB	Coleiro and Chaty (2013)
RXJ1037.5-5648	5.0	HMXB	Grimm et al. (2002)
SctX-1	10.0	HMXB	Grimm et al. (2002)
X1630-472	4.0	LMXB	Grimm et al. (2002)
X0042+327	7.0	LMXB	Grimm et al. (2002)
X0142+614	1.0	LMXB	Grimm et al. (2002)
X0614+091	3.0	LMXB	Grimm et al. (2002)
X1543-624	10.0	LMXB	Grimm et al. (2002)
X1553-542	10.0	HMXB	Grimm et al. (2002)
X1556-605	10.0	LMXB	Grimm et al. (2002)
X1627-673	8.0	LMXB	Grimm et al. (2002)
X1730-333	8.0	LMXB	Grimm et al. (2002)
X1755-338	6.0	LMXB	Grimm et al. (2002)
X1803-245	8.0	LMXB	Grimm et al. (2002)
X1822-000	4.0	LMXB	Grimm et al. (2002)
X1822-371	2.5	LMXB	Grimm et al. (2002)
X1957+115	7.0	LMXB	Grimm et al. (2002)
X2129+470	2.2	LMXB	Grimm et al. (2002)
XTEJ0421+560	1.0	HMXB	Grimm et al. (2002)
1E1048.1-5937	3.0	HMXB	Grimm et al. (2002)
1E1740.7-2942	8.5	LMXB	Grimm et al. (2002)
1E2259.0+5836	4.0	LMXB	Grimm et al. (2002)
GCX-1	8.5	LMXB	Grimm et al. (2002)
GS0834-430	7.1	HMXB	Coleiro and Chaty (2013)
GRS1739-278	6.0	LMXB	Grimm et al. (2002)
GRS1758-258	8.5	LMXB	Grimm et al. (2002)

**Appendix: Distances to X ray binaries(continued)**

X ray sources	Distance	Type	References
GX1+4	10.0	LMXB	Grimm et al. (2002)
X0512-401	12.2	LMXB	Liu et al. (2007)
X0921-630	7.0	LMXB	Liu et al. (2007)
X1246-588	5.0	LMXB	Liu et al. (2007)
SAXJ1324.5-6313	6.2	LMXB	Liu et al. (2007)
X1524-617	4.4	LMXB	Liu et al. (2007)
MS1603.6+2600	5.0	LMXB	Liu et al. (2007)
X1711-339	7.5	LMXB	Liu et al. (2007)
SAXJ2224.9+5421	7.1	LMXB	Liu et al. (2007)
GRS1737-31	8.5	LMXB	Liu et al. (2007)
EXO1747-214	11.0	LMXB	Liu et al. (2007)
XTEJ1748-288	8.0	LMXB	Liu et al. (2007)
SAXJ1752.3-3128	9.0	LMXB	Liu et al. (2007)
SWIFTJ1753.5-0127	6.0	LMXB	Liu et al. (2007)
SAXJ1806.5-2215	8.0	LMXB	Liu et al. (2007)
XTEJ1817-330	1.0	LMXB	Liu et al. (2007)
SAXJ1818.7+1424	9.4	LMXB	Liu et al. (2007)
X1850-087	8.2	LMXB	Liu et al. (2007)
XTEJ1908+094	3.0	LMXB	Liu et al. (2007)
X1953+319	1.7	LMXB	Liu et al. (2007)
SAXJ0635+0533	2.5	HMXB	Liu et al. (2006)
XTEJ1739-302	2.3	HMXB	Liu et al. (2006)
AXJ1841-0536	10.0	HMXB	Liu et al. (2006)
X1901+031	10.0	HMXB	Liu et al. (2006)
XTEJ1906+09	10.0	HMXB	Liu et al. (2006)
GROJ2058+42	9.0	HMXB	Liu et al. (2006)
SAXJ2239.3+6116	4.4	HMXB	Liu et al. (2006)
HerX-1	6.6	LMXB	Reynolds et al. (1997)
EXO1722-363	8.0	HMXB	Bodaghee et al. (2012)
X1704+240	0.42	LMXB	Liu et al. (2007)
RXJ1709.5-2639	11.0	LMXB	Liu et al. (2007)
X2127+119	5.8	LMXB	Galloway et al. (2008)